

k -meansNet: When k -means Meets Differentiable Programming

Xi Peng, Joey Tianyi Zhou, and Hongyuan Zhu

Abstract—In this paper, we study how to make clustering benefiting from differentiable programming whose basic idea is treating the neural network as a language instead of a machine learning method. To this end, we recast the vanilla k -means as a novel feedforward neural network in an elegant way. Our contribution is two-fold. On the one hand, the proposed k -meansNet is a neural network implementation of the vanilla k -means, which enjoys four advantages highly desired, *i.e.*, robustness to initialization, fast inference speed, the capability of handling new coming data, and provable convergence. On the other hand, this work may provide novel insights into differentiable programming. More specifically, most existing differentiable programming works unroll an **optimizer** as a **recurrent neural network**, namely, the neural network is employed to solve an existing optimization problem. In contrast, we reformulate the **objective function** of k -means as a **feedforward neural network**, namely, we employ the neural network to describe a problem. In such a way, we advance the boundary of differentiable programming by treating the neural network as from an alternative optimization approach to the problem formulation. Extensive experimental studies show that our method achieves promising performance comparing with 12 clustering methods on some challenging datasets.

Index Terms—Subspace Clustering, Low Rank Representation, Least Square Regression, Model based Optimization, Learning-based iteration, Convergence

1 INTRODUCTION

CLUSTERING is one of most fundamental tasks in machine learning and computer vision, which aims to group similar patterns into the same cluster and dissimilar patterns into different clusters. During past decades, a variety of clustering methods [1] have been proposed and achieved huge success in various applications. In recent, the major focus of the community is paid on handling high-dimensional data whose key is addressing the linear inseparable challenge. To solve this issue, one of the most popular methods is subspace clustering [2].

Subspace clustering implicitly seeks a set of low-dimensional subspaces and clusters the data into these subspaces. The typical methods include algebraic approach [3], [4], iterative approach [5], statistical approach [6], and spectral clustering based approach [7], [8]. In recent, spectral clustering based subspace clustering has earned a lot of interests from the community, which mainly consists of two steps, namely, representation learning and clustering. More specifically, the data are projected into a latent space via representation learning and then the data clustering is obtained by conducting the vanilla k -means on the representation.

According to the used representation learning approach, existing spectral clustering based subspace clustering methods could be divided into two categories, *i.e.*, shallow and deep method. In short, the shallow methods such as sparse

subspace clustering [9], [10], low rank representation [11], [12], ℓ_2 -norm based methods [13], and their variants [12], [14]–[21] represent each data point as a linear/nonlinear combination of the whole data set with different regularizations and then use the representation coefficients to build a graph Laplacian for dimension reduction. Clearly, these two steps could be regarded as identical to the well-known manifold learning [22]. Different from shallow methods, deep clustering methods [23]–[26] employ deep neural networks instead of manifold learning to obtain a discriminative representation, which have achieved state-of-the-art performance in data clustering.

Despite the success of existing subspace clustering methods including shallow and deep ones, they mainly focus on representation learning while ignoring the clustering side. In the era of deep learning, it is highly desirable to pay more attention to developing new clustering algorithms since deep neural networks have shown promising performance in learning representation. Furthermore, to embrace the smooth collaboration with deep representation learning, it is preferable to implement clustering through a neural network.

Motivated by the above observation, this paper proposes a novel neural network (see Fig. 1) which is a reformulation of the vanilla k -means clustering with following advantages. First, k -means iteratively optimizes the cluster centers and the label assignments with two separate steps, which leads to the slow inference speed and the incapability of handling new coming data [27]. In contrast, the proposed k -meansNet simultaneously learns a set of cluster centers and the label assignments which correspond to the weight and output of our neural network. Benefiting from the neural network implementation, the proposed k -meansNet could enjoy fast inference speed and the capability of handling new data

- X. Peng is with College of Computer Science, Sichuan University, Chengdu, 610065, China.
E-mail: pengx.gm@gmail.com
- J. Zhou is with Institute of High Performance Computing, A*STAR, Singapore.
E-mail: joey.tianyi.zhou@gmail.com
- H. Zhu is with Institute for Infocomm Research, A*STAR, Singapore.
Email: hongyuanzhu.cn@gmail.com

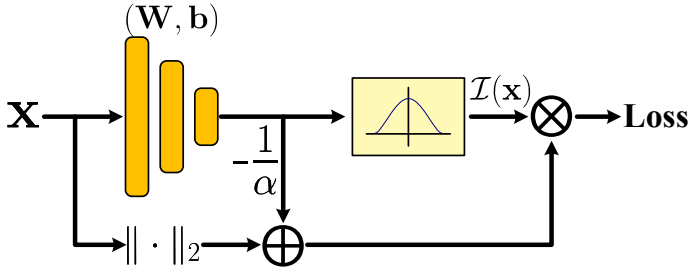


Fig. 1. An illustration on the proposed k -meansNet. In the figure, \mathbf{x} denotes a given input, α is a parameter, $\mathcal{I}(\mathbf{x})$ denotes the label assignment of \mathbf{x} , $\mathbf{W}_i = 2\alpha\Omega_i$, $\mathbf{b}_i = -\alpha\|\Omega_i\|_2^2$, and Ω_i denotes the i -th cluster center. The used activation function normalizes an input into the range of $[0, 1]$, e.g., the *softmax* function. Note that, if enforcing $\|\mathbf{x}_i\|_2^2 = 1$, the norm operator $\|\cdot\|_2$ could be removed.

which are intrinsic properties rooted in neural networks. Furthermore, we experimentally show that k -meansNet is robust to different initialization approaches highly desired by k -means. Second, it is more feasible to employ our neural network as a component to integrate with other deep learning techniques since they could be smoothly stacked together and jointly optimized by various SGD optimizers. Note that, end-to-end learning is commonly regarded as one major reason to the huge success of deep learning [28]. Third, our method is provable to monotonically decreasing in the loss under mild conditions. To the best of our knowledge, this could be one of the first attempts to develop a novel clustering method in differentiable programming (DP)¹.

“Deep Learning est Mort! Vive Differentiable Programming” by Yann Lecun. Our work belongs to the family of differentiable programming or called model-based optimization in recent literature [29]–[35]. The basic idea of differentiable programming is treating the neural network as a language instead of a machine learning method. In literature, these pioneers unroll an optimization method as a recurrent neural network (RNN) since the mathematics behind the optimization and RNN is a dynamic system, i.e., an iterative equation. Benefiting from this fact, algorithm-based optimization is transformed into model-based one, thus simultaneously enjoying high interpretability of traditional machine learning method and good performance of neural networks. Among existing works, the most related method could be [30] which unfolds an ℓ_1 -regularized optimization into a recurrent neural network (RNN) to learn clustering-specific features. Our work is substantially different from these existing works including [30] from following aspects. First, the network is different. More specifically, almost all these methods will obtain a *recurrent* neural network, whereas our k -meansNet is a *feedforward* neural network (FNN) which is an equivalent reformulation of k -means. Second, the idea is different. In short, these existing works reformulate the *optimization* process as an RNN, whereas we recast and encapsulate the *objective function* into a neural network for data clustering. In other words, these existing

works treat the neural network as an alternative optimization method, whereas our work employs the neural network as a language to describe the physical model. Third, [30] proposes a task-specific recurrent architecture derived from sparse coding domain expertise, as well as the joint optimization with clustering-oriented loss functions. In contrast, we only focus on data clustering via a novel neural network derived from the vanilla k -means. As a result, our network enjoys a higher feasibility than [30] since it is independent of any feature extraction modules.

The contribution of this work is twofold. From the view of clustering, we explicitly reformulate k -means as a neural network with novel objective function in an elegant way, thus overcoming the drawbacks of k -means and enjoying the advantages of neural networks. From the view of differentiable programming, this work advances its boundary from the *optimization process* to the *objective function* and from the *recurrent neural network* to the *feedforward neural network*. In other words, this work does not employ the neural network as an alternative optimization approach as existing DP works did. As such a difference is more consistent with the original intention of differentiable programming (as a language), novel insights may be provided to the communities of clustering and differentiable programming.

2 RELATED WORKS

This work closely relates to subspace clustering and differentiable programming which are briefly discussed in this section.

2.1 Subspace Clustering

With different choices in representation learning technique, most popular subspace clustering methods fall into two categories, namely, shallow subspace clustering and deep subspace clustering. For a given data set $\mathbf{X} = \{\mathbf{x}_1, \mathbf{x}_2, \dots, \mathbf{x}_n\}$, shallow methods first compute a so-called self-expression $\mathbf{C} \in \mathcal{R}^{n \times n}$ by

$$\min \|\mathbf{X} - \mathbf{XC}\|_F^2 + \mathcal{R}(\mathbf{C}) + \mathcal{Q}(\mathbf{C}), \quad (1)$$

where $\mathbf{x} \in \mathcal{R}^m$, $\mathcal{R}(\mathbf{C})$ is the adopted regularization term, and $\mathcal{Q}(\mathbf{C})$ denotes some desirable constraints.

The main difference among these shallow methods lies on the choice of $\mathcal{R}(\mathbf{C})$ and $\mathcal{Q}(\mathbf{C})$. In practice, there are several popular forms of $\mathcal{R}(\mathbf{C})$, namely, ℓ_0 -norm [10], ℓ_1 -norm [9], ℓ_2 -norm [13], [36], nuclear-norm [11], and their variants [12], [14]–[16], [37]–[39]. After obtaining \mathbf{C} , a graph Laplacian is computed based on \mathbf{C} and the data partitions are given by conducting k -means on the top eigenvectors of the Laplacian matrix. Different from shallow methods, deep subspace clustering [23], [26] utilize a neural network to learn features and then employ k -means or spectral clustering in the feature space.

Different from these existing works, we aim to develop a novel neural network to achieve clustering rather than representation learning. More importantly, we recast k -means as an independent component that could be integrated with other deep learning techniques, while embracing the fast inference speed and capacity of handling new coming data inherently rooted in neural networks.

1. Note that, neural gas employs competitive learning for clustering, which seems like k -means but they are totally different in the motivation and methodology.

2.2 Differentiable Programming

To the best of our knowledge, Learned ISTA (LISTA) [29] could be the first well-known work of differentiable programming in the era of deep learning, which unfolds the ISTA [40] – a popular ℓ_1 -optimizer, as a simple RNN wherein the number of layers corresponds to the iteration number and the weight corresponds to the dictionary. Inspired by the success of LISTA, numerous methods are proposed to address a variety of problems, *e.g.* image deblurring [31] and restoration [41], audio processing [32], image segmentation [33], visual analysis [34], and data clustering [30]. The key idea behind them is treating the neural network as a programming language instead of a machine learning method. Benefiting from the neural network based formulation, ideally, any machine learning methods could be recast as a neural network and thus embrace high desirable advantages of deep learning and statistical machine learning.

As discussed in Introduction, this work is remarkably different from most existing differentiable programming approaches in either network structure (RNN vs. FNN) or basic idea (optimization reformulation vs. loss reformulation).

3 NEURAL NETWORK BASED k -MEANS CLUSTERING

In this section, we first show how to reformulate k -means as a neural network and then conduct convergence analysis on the proposed k -meansNet.

3.1 Formulation

For a given data set $\mathbf{X} = \{\mathbf{x}_1, \mathbf{x}_2, \dots, \mathbf{x}_n\}$, k -means aims to partition it into $k \leq n$ different sets $\mathcal{S} = \{\mathcal{S}_1, \mathcal{S}_2, \dots, \mathcal{S}_k\}$ by minimizing the distance of the data points that belong to the same cluster. In mathematical,

$$\operatorname{argmin}_{\mathcal{S}} \sum_j \sum_{\mathbf{x} \in \mathcal{S}_j} \|\mathbf{x} - \boldsymbol{\Omega}_j\|_2^2, \quad (2)$$

where $\boldsymbol{\Omega}_j$ is the j -th cluster center which is computed as the mean of points in \mathcal{S}_j , *i.e.*,

$$\boldsymbol{\Omega}_j = \frac{1}{|\mathcal{S}_j|} \sum_{\mathbf{x}_i \in \mathcal{S}_j} \mathbf{x}_i, \quad (3)$$

where $|\mathcal{S}_j|$ denotes the number of data points in the j -th cluster.

To solve Eq.(2), an EM-like optimization is adopted by updating $\mathcal{I}(\mathbf{x})$ or $\boldsymbol{\Omega}$ and simultaneously fixing the other one. Such an iterative optimization has several drawbacks. First, the method is sensitive to the initialization, which may achieve an inferior result for a given bad initialized $\boldsymbol{\Omega}$. In fact, to obtain a stable solution, over-thousands of works have been conducted, including the popular k -means++ [42]. Second, it is an NP-hard problem to finding the optimal solution to k -means in either of general Euclidean space m even for bi-cluster and in the plane for a general number of k . To solve the NP-hard problem, some variants of k -means are proposed, such as various parametric k -means including Fuzzy c -means (FCM) [43],

[44]. Third, k -means cannot handle the new coming data, which requires the whole data set is observed. Furthermore, for fixed k and m , the complexity of k -means is $O(n^{mk+1})$.

To overcome these disadvantages, we recast k -means as a novel neural network. To this end, we first rewrite Eq.(2) as follows:

$$\min \sum_{i=1}^n \sum_{j=1}^k \mathcal{I}_j(\mathbf{x}_i) \|\mathbf{x}_i - \boldsymbol{\Omega}_j\|_2^2, \quad (4)$$

where $\mathcal{I}_j(\mathbf{x}_i)$ indicates the cluster membership of \mathbf{x}_i *w.r.t.* $\boldsymbol{\Omega}_j$ and only one entry of $\mathcal{I}_j(\mathbf{x}_i)$ is nonzero. In the following, we will alternatively use \mathcal{I}_{ij} to denote $\mathcal{I}_j(\mathbf{x}_i)$ for simplicity.

The binary constraint on \mathcal{I}_{ij} will lead to a NP-hard problem as the aforementioned. Hence, we relax such a constraint and define \mathcal{I}_{ij} as a probability map based on the distance between \mathbf{x}_i and $\boldsymbol{\Omega}_j$, *i.e.*,

$$\mathcal{I}_j(\mathbf{x}_i) = \frac{\exp(-\alpha \|\mathbf{x}_i - \boldsymbol{\Omega}_j\|_2^2)}{\sum_j \exp(-\alpha \|\mathbf{x}_i - \boldsymbol{\Omega}_j\|_2^2)}, \quad (5)$$

where $\alpha > 0$ is the normalization factor. Note that, here we adopt the *softmax* function. However, other activation functions could also be used as long as \mathcal{I}_{ij} is normalized into the range of $[0.0, 1.0]$. It is worthy to point out that replacing the hard indicator of k -means with the *softmax* function is not the key contribution of our idea. Instead, the major novelty of this work is recasting k -means as a neural network via following reformulation,

$$-\alpha \|\mathbf{x}_i - \boldsymbol{\Omega}_j\|_2^2 = -\alpha \|\mathbf{x}_i\|_2^2 + 2\alpha \boldsymbol{\Omega}_j^\top \mathbf{x}_i - \alpha \|\boldsymbol{\Omega}_j\|_2^2. \quad (6)$$

Let $\mathbf{W} = 2\alpha \boldsymbol{\Omega}$, $\mathbf{b}_j = -\alpha \|\boldsymbol{\Omega}_j\|_2^2$, and $\|\mathbf{x}_i\|_2^2 = 1$ without loss of generality², the objective function of k -meansNet is formulated as below:

$$\mathcal{L} = \sum_{ij} \mathcal{L}_{ij} = \sum_{ij} \mathcal{I}_{ij} \left(-\frac{1}{\alpha} \mathbf{W}_j^\top \mathbf{x}_i - \frac{1}{\alpha} \mathbf{b}_j \right), \quad (7)$$

$$\mathcal{I}_{ij} = \frac{\exp(\mathbf{W}_j^\top \mathbf{x}_i + \mathbf{b}_j)}{\sum_j \exp(\mathbf{W}_j^\top \mathbf{x}_i + \mathbf{b}_j)}, \quad (8)$$

where \mathbf{b}_j is a scalar which denotes the j -th entry of \mathbf{b} and $\boldsymbol{\Omega}_i$ denotes the i -th cluster center.

Such a reformulation corresponds to a single-layer neural network as demonstrated in Fig. 1. It should be pointed out that, \mathbf{W} and \mathbf{b} will be decoupled during training to favor an additional free degree and avoiding trivial solutions as proved later. In other words, after initialization with $\boldsymbol{\Omega}$, \mathbf{W} and \mathbf{b} are updated independently and the final cluster centers $\boldsymbol{\Omega}^*$ is recovered via $\boldsymbol{\Omega}^* = \frac{1}{2\alpha} \mathbf{W}^*$.

To show the necessity of decoupling \mathbf{W} and \mathbf{b} , similar to the above reformulation process, we rewrite Eqn.(7) as

$$\begin{aligned} \mathcal{L} &= -\frac{1}{\alpha} \sum_i \sum_j \frac{\exp(\mathbf{b}_j + \mathbf{W}_j^\top \mathbf{x}_i - \alpha)(\mathbf{b}_j + \mathbf{W}_j^\top \mathbf{x}_i - \alpha)}{\sum_k \exp(\mathbf{b}_k + \mathbf{W}_k^\top \mathbf{x}_i - \alpha)} \\ &= -\frac{1}{\alpha} \sum_i \frac{\sum_j \exp(\mathbf{z}_j) \mathbf{z}_j}{\sum_k \exp(\mathbf{z}_k)} = -\frac{1}{\alpha} \sum_i f(\mathbf{z}_i), \end{aligned} \quad (9)$$

2. Noticed that, this reformulation is one major contribution of this work.

where $\mathbf{z}_j = (-\frac{\|\mathbf{W}_j\|_2^2}{4\alpha} + \mathbf{W}_j^\top \mathbf{x}_i - \alpha)$ (for simplicity, we drop the subscript i for \mathbf{x}_i). Thus, we have

$$\begin{aligned} \mathcal{L} &= -\frac{1}{\alpha} f(\mathbf{z}) \\ \text{s.t. } \mathbf{z}_j &= -\frac{\|\mathbf{W}_j\|_2^2}{4\alpha} + \mathbf{W}_j^\top \mathbf{x}_i - \alpha, \quad \|\mathbf{W}_j\|_2 \leq 2\alpha. \end{aligned} \quad (10)$$

Eqn.(10) is exact to Eqn.(5), namely, without the decoupling of \mathbf{W} and \mathbf{b} . Since $f(\mathbf{z})$ obtains its maximal value at the boundary with $\mathbf{z}_1 = \mathbf{z}_2 = \dots$ and $f(\mathbf{z}) = \infty$ when $\mathbf{z} = \infty$, there exists z such that $\mathbf{z}_j = z$ and $f(\mathbf{z})$ obtains its maximal value. We can always find a \mathbf{W}_j and \mathbf{b}_j such that $\mathbf{b}_j + \mathbf{W}_j^\top \mathbf{x} - \alpha = z$, however, we cannot always find a \mathbf{W}_j and \mathbf{b}_j such that $-\frac{\|\mathbf{W}_j\|_2^2}{4\alpha} + \mathbf{W}_j^\top \mathbf{x}_i - \alpha = z$. In other words, we have to decouple \mathbf{W}_j and \mathbf{b}_j during training.

3.2 Convergence Proofs

In this section, we theoretically show that the loss \mathcal{L} given by our k -meansNet will sufficiently converge to the optimizers.

Without loss of generality, the basis \mathbf{b} could be enveloped into the weight \mathbf{W} via $\mathbf{W}^\top = [\mathbf{W}^\top \mathbf{b}]$ and $\mathbf{x}_i = [\mathbf{x}_i^\top 1]^\top$. For ease of presentation, let \mathcal{L}^* denote the smallest loss, and \mathcal{L}_t^* be the smallest loss found at the t -step so far. Similarly, \mathbf{W}^* denotes the desirable weight of which the first k columns are the optimal cluster centers Ω^* . We consider the standard SGD to optimize our network, i.e.,

$$\mathbf{W}_{t+1} = \mathbf{W}_t - \eta_t \nabla \mathcal{L}(\mathbf{W}_t), \quad (11)$$

where $\nabla \mathcal{L}(\mathbf{W}_t)$ denotes the gradient of \mathcal{L} w.r.t. \mathbf{W}_t . In the following, we will alternatively use $\nabla \mathcal{L}(\mathbf{W}_t)$ and $\nabla \mathcal{L}_t$ without causing confusion.

Definition 1 (Lipschitz Continuity). A function $f(x)$ is a Lipschitz continuous function on the set Ω , if there exists a constant $\epsilon > 0$, $\forall x_1, x_2 \in \Omega$ such that

$$\|f(x_1) - f(x_2)\| \leq \epsilon \|x_1 - x_2\|, \quad (12)$$

where ϵ is termed as the Lipschitz constant.

Clearly, our objective function \mathcal{L} is a Lipschitz continuous function i.i.f. $\|\nabla \mathcal{L}_t\| \leq \epsilon$. In other words, we need to prove the existence of upper boundary of $\nabla \mathcal{L}_t$ for utilizing the Lipschitz Continuity.

Theorem 1. There exists $\epsilon > 0$ such that $\|\nabla \mathcal{L}_t\| \leq \epsilon$.

Proof. Without loss of generality, Eqn.(7) could be rewritten in the form of

$$\mathcal{L}(\mathbf{W}) = \sum_j \frac{\sum_i \exp(\mathbf{W}_i^\top \mathbf{x}_j) \mathbf{W}_i^\top \mathbf{x}_j}{\sum_k \exp(\mathbf{W}_k^\top \mathbf{x}_j)}. \quad (13)$$

Let $\mathbf{z}_i = \mathbf{W}_i^\top \mathbf{x}_j$, we have

$$f(\mathbf{z}_i) = \frac{\sum_i \exp(\mathbf{z}_i) \mathbf{z}_i}{\sum_j \exp(\mathbf{z}_j)} = \mathbf{p}_i \mathbf{z}_i, \quad (14)$$

then

$$\begin{aligned} \nabla_i f(\mathbf{z}_i) &= \frac{(\exp(\mathbf{z}_i) + \exp(\mathbf{z}_i) \mathbf{z}_i) \sum_j \exp(\mathbf{z}_j)}{(\sum_j \exp(\mathbf{z}_j))^2} \\ &\quad - \frac{\exp(\mathbf{z}_i) \sum_j \exp(\mathbf{z}_j) \mathbf{z}_j}{(\sum_j \exp(\mathbf{z}_j))^2} \\ &= \mathbf{p}_i + \mathbf{p}_i \mathbf{z}_i - \mathbf{p}_i \mathbf{p}_j \mathbf{z}_j. \end{aligned} \quad (15)$$

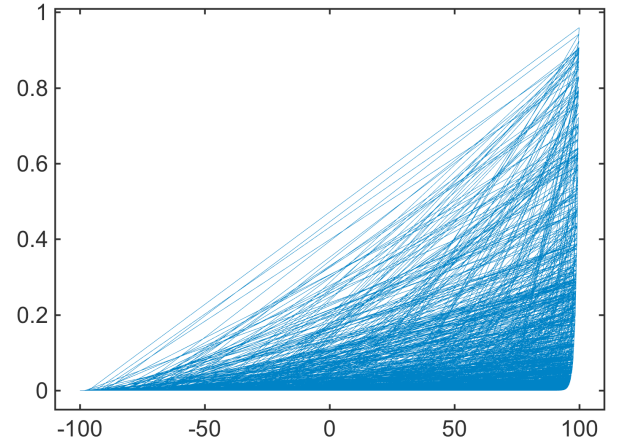


Fig. 2. A toy example to show the boundness of our loss function in 1-dimensional case. x-axis denotes the data points (\mathbf{z}) randomly sampled from -100 to 100, and y-axis denotes the corresponding loss $\frac{\exp(\mathbf{z})\mathbf{z}}{\sum_i \exp(\mathbf{z})}$. One could see that our loss function will be bounded if \mathbf{z} is bounded.

As $0 \leq \|\mathbf{p}_i\| \leq 1$, we could further have

$$\begin{aligned} \|\nabla_i f(\mathbf{z}_i)\| &\leq \|\mathbf{p}_i\| (1 + \|\mathbf{z}_i\| + \mathbf{p}_j \|\mathbf{z}_j\|) \\ &\leq 1 + \|\mathbf{z}_i\| + \|\mathbf{z}_j\|. \end{aligned} \quad (16)$$

Clearly our objective function $\mathcal{L}(\mathbf{W})$ will be upper bounded by a positive real number ϵ when $\|\mathbf{z}_i\|$ is bounded (see Fig. 2 for an illustrative example). In fact, there exists the upper boundary of $\|\mathbf{z}_i\|$ due to $\|\mathbf{x}_i\| = 1$ and $\|\mathbf{W}\| \leq 2\alpha$ induced by $\mathbf{W}_i = 2\alpha \Omega_i = \frac{2\alpha}{|\mathcal{S}_i|} \sum_{\mathbf{x}_j \in \mathcal{S}_i} \mathbf{x}_j$, where $|\mathcal{S}_i|$ denotes the size of the i -th cluster. \square

Based on Theorem 1, we could have following convergence result by following [45].

Theorem 2. One could always find an optimal model \mathcal{L}_T^* which is sufficiently close to the desired \mathcal{L}^* after T steps, i.e.,

$$\mathcal{L}_T^* - \mathcal{L}^* \leq \frac{\|\mathbf{W}_1 - \mathbf{W}^*\|_F^2 + \epsilon^2 \sum_{t=1}^T \eta_t^2}{2 \sum_{t=1}^T \eta_t} \quad (17)$$

Proof. Let $\mathbf{W}^* = 2\alpha \Omega^*$ be the minimizer to our objective function (i.e., Eqn.(7)), then

$$\begin{aligned} \|\mathbf{W}_{T+1} - \mathbf{W}^*\|_F^2 &= \|\mathbf{W}_T - \mathbf{W}^*\|_F^2 \\ &\quad - 2tr(\eta_T \nabla \mathcal{L}_T^\top (\mathbf{W}_T - \mathbf{W}^*)) + \eta_T^2 \|\nabla \mathcal{L}_T\|_F^2, \end{aligned} \quad (18)$$

where $tr(\cdot)$ denotes the trace of a matrix.

Applying the above Equation recursively, it gives that

$$\begin{aligned} \|\mathbf{W}_{T+1} - \mathbf{W}^*\|_F^2 &= \|\mathbf{W}_1 - \mathbf{W}^*\|_F^2 \\ &\quad - 2 \sum_{t=1}^T \eta_t tr(\mathbf{W}_t - \mathbf{W}^*) + \sum_{t=1}^T \eta_t^2 \|\nabla \mathcal{L}_t\|_F^2. \end{aligned} \quad (19)$$

As $\mathcal{L}(\mathbf{W})$ satisfies the Lipschitz Continuity and according to the definition of gradient, i.e.,

$$f(x^*) \geq f(x_t) + \nabla \mathcal{L}_t^\top (x^* - x_t) \quad (20)$$

then,

$$\|\mathbf{W}_{T+1} - \mathbf{W}^*\|_F^2 \leq \|\mathbf{W}_1 - \mathbf{W}^*\|_F^2 - 2 \sum_{t=1}^T \eta_t (\mathcal{L}_t - \mathcal{L}^*) + \epsilon^2 \sum_{t=1}^T \eta_t^2. \quad (21)$$

Clearly,

$$2 \sum_{t=1}^T \eta_t (\mathcal{L}_t - \mathcal{L}^*) \leq \|\mathbf{W}_1 - \mathbf{W}^*\|_F^2 + \epsilon^2 \sum_{t=1}^T \eta_t^2. \quad (22)$$

Since

$$\mathcal{L}_t - \mathcal{L}^* \geq \min_{t=1,2,\dots,T} (\mathcal{L}_t - \mathcal{L}^*) = \mathcal{L}_T^* - \mathcal{L}^*, \quad (23)$$

where \mathcal{L}_T^* is the best \mathcal{L} found within T steps so far.

Combining Eqn.(22) and Eqn.(23), it gives that

$$\mathcal{L}_T^* - \mathcal{L}^* \leq \frac{\|\mathbf{W}_1 - \mathbf{W}^*\|_F^2 + \epsilon^2 \sum_{t=1}^T \eta_t^2}{2 \sum_{t=1}^T \eta_t} \quad (24)$$

as desired. \square

Based on Theorem 2, the following two lemmas could be derived.

Lemma 1. For the fixed step size (i.e. $\eta_t = \eta$) and $T \rightarrow \infty$,

$$\mathcal{L}_T^* - \mathcal{L}^* \rightarrow \frac{\eta \epsilon^2}{2} \quad (25)$$

Proof. After T steps, we have

$$\begin{aligned} \mathcal{L}_T^* - \mathcal{L}^* &\leq \frac{\|\mathbf{W}_1 - \mathbf{W}^*\|_F^2 + T \epsilon^2 \eta^2}{2T\eta} \\ &= \frac{\|\mathbf{W}_1 - \mathbf{W}^*\|_F^2 / (T\eta) + \eta \epsilon^2}{2} \end{aligned} \quad (26)$$

as desired. \square

Lemma 2. For the fixed step length (i.e. $\eta_t = \eta / \nabla \mathcal{L}_t$) and $T \rightarrow \infty$,

$$\mathcal{L}_T^* - \mathcal{L}^* \rightarrow \frac{\eta \epsilon}{2} \quad (27)$$

Proof. Similar to the proof for Lemma 1. \square

Lemmas 1-2 show that the loss will sufficiently converge to \mathcal{L}^* with a radius of $\frac{\eta \epsilon^2}{2}$ and $\frac{\eta \epsilon}{2}$ within T steps.

4 EXPERIMENTAL RESULTS

In this section, we carry out experiments to verify the effectiveness of the proposed k -meansNet comparing with 12 state-of-the-art clustering approaches.

4.1 Experimental Settings

We conduct experiments on a Nvidia K40 GPU, an Intel Xeon CPU 2.40GHz, and a 64GB memory. For all the tested baselines, we use the source code released by respective authors. Regarding our method, we implement it in TensorFlow.

Baselines: We compare our method with 1) popular subspace clustering approaches including spectral clustering (SC) [7], LRR [11], and LSR [13]; 2) large-scale clustering methods including Scalable LRR (SLRR) [27] and large-scale spectral clustering (LSC) [46]; 3) matrix decomposition based method and agglomerative clustering, i.e., NMF-LP [47] and Zeta function based agglomerative clustering (ZAC) [48]; and 4) state-of-the-art deep embedding clustering (DEC) [24]. Moreover, we also use the vanilla k -means and FCM [44] as baselines. Note that, either of LSR and LSC

has two variants, which are denoted by LSR1, LSR2, LSC-R, and LSC-K.

In experiments, we employ an auto-encoder as the feature extractor stacked on k -means, FCM, and our k -meansNet to show their compatibility with deep representation learning techniques. To be specific, like DEC [24], the auto-encoder consists of an encoder with the fully connected layers (FCL) of m -(500)-(500)-(2000)-(10) and a decoder with the fully connected layers of (2000)-(500)-(500)-(m), where Z in (Z) represents fully connected layer with Z number of neurons and m is the input dimension. We adopt the *ReLU* as the activation function for all layers except the last one of encoder and decoder which is with the *sigmoid* function. To alleviate the overfitting, a dropout layer with the rate of 0.2 is added after each layer of the encoder. The adadelta [49] optimizer is used to train the neural networks including the auto-encoder and k -meansNet. Either of the max training epoch and convergence error is satisfied, the neural network is regarded as convergent. In all experiments, these two parameters are fixed to 3000 and 10^{-3} . Furthermore, for fair comparisons, we tune parameters for all tested methods and report their best performance. For the baselines, we follow the parameter ranges suggested in original work. For our method, we only tune α ranged into $\{1, 5\} \times 10^p$, where p increases from -5 to 0 .

Datasets: Following data sets are used to evaluate the performance of our method, including the mnist handwritten digital full database [50], the CIFAR10 image full database [51], and the CIFAR100 full database [51]. For CIFAR100, we adopt superclass partitions. In other words, we conduct experiments on 20 supersets of CIFAR100 and report the mean, the median, and the maximum of result over these subsets.

Evaluation Metrics: Three metrics are used to evaluate the clustering performance, i.e., Accuracy or called Purity, normalized mutual information (NMI), and adjusted rand index (ARI). A higher value of these metrics indicates better clustering performance.

4.2 Experimental Comparisons

In this section, we examine the performance of k -meansNet on three challenging data sets. As all tested methods excepted ZAC directly/indirectly involve initialization of cluster centers, we adopt k -means++ as the initializer for fair comparisons. For our method, k -means++ first initialize Ω which is further used to compute $\{\mathbf{W}, \mathbf{b}\}$.

The mnist consists of 70,000 images distributed over 10 handwritten digits and each image is with the size of 28×28 . The CIFAR10 dataset consists of 60,000 images sampled from 10 classes and each image is with the size of $32 \times 32 \times 3$. Table 1 demonstrates the results of the evaluated approaches on these two data sets. One could observe that k -meansNet is superior to all baselines in terms of three metrics and DEC achieves the second best result. For example, our method outperforms the second best approach 4.11%, 5.10%, and 6.61% on mnist *w.r.t.* Accuracy, NMI, and ARI thanks to the new reformulation and neural network based implementation. Note that, LRR and SLRR show inferior performance in experiments, and the possible reason is that these data sets do not satisfy the low-rank assumption well.

TABLE 1
Clustering results on the **mnist** and the **CIFAR10** full data set.

Methods	mnist				CIFAR10			
	Accuracy	NMI	ARI	Parameter	Accuracy	NMI	ARI	Parameter
k-means	78.32%	77.75%	70.53%	-	19.81%	5.94%	3.01%	-
FCM	21.56%	12.39%	5.10%	-	17.02%	3.92%	2.56%	-
SC	71.28%	73.18%	62.18%	1	19.81%	4.72%	3.22%	10
LRR	21.07%	10.43%	10.03%	10.01	13.07%	0.43%	0.03%	0.01
LSR1	40.42%	31.51%	21.35%	0.4	19.79%	6.05%	3.64%	0.6
LSR2	41.43%	30.03%	20.00%	0.1	19.08%	6.37%	3.16%	0.5
SLRR	21.75%	7.57%	5.55%	2.1	13.09%	1.31%	0.94%	0.1
LSC-R	59.64%	56.68%	45.98%	6	18.39%	5.67%	2.58%	3
LSC-K	72.07%	69.88%	60.81%	6	19.29%	6.34%	3.89%	3
NMF-LP	46.35%	43.58%	31.20%	10	19.68%	6.20%	3.21%	3
ZAC	60.00%	65.47%	54.07%	20	5.24%	0.36%	0.00%	10
DEC	83.65%	73.60%	70.10%	10	18.09%	4.56%	2.47%	80
k-meansNet	87.76%	78.70%	76.71%	1.00E-03	20.23%	6.87%	3.95%	0.5

TABLE 2
Clustering **Accuracy** (%) on the first 10 supersets of the **CIFAR100** data set.

Methods	s1	s2	s3	s4	s5	s6	s7	s8	s9	s10	max	mean	median
<i>k</i> -means	29.63	43.30	31.53	30.03	34.83	30.43	33.60	38.80	28.93	30.70	43.30	33.18	31.12
FCM [44]	26.77	37.80	25.30	25.97	29.77	26.37	32.60	36.73	25.00	25.33	37.80	29.16	26.57
SC [7]	31.90	39.30	33.67	27.53	34.27	27.77	33.10	36.17	26.90	32.30	39.30	32.29	32.70
LRR [11]	21.77	21.73	21.37	20.13	21.60	21.80	21.53	21.27	21.90	21.50	21.90	21.46	21.57
LSR1 [13]	21.93	21.40	22.27	21.87	21.47	21.30	22.33	21.97	21.07	21.90	22.33	21.75	21.89
LSR2 [13]	22.93	22.67	22.87	23.80	24.10	21.83	22.07	25.30	21.77	22.10	25.30	22.94	22.77
SLRR [27]	22.40	22.27	21.77	21.73	22.50	22.63	22.53	22.57	22.40	22.50	22.63	22.33	22.45
LSC-R [46]	31.97	40.50	30.77	28.87	34.30	28.67	32.90	35.27	27.13	32.03	40.50	32.24	32.00
LSC-K [46]	32.36	39.97	34.30	30.93	34.37	30.07	32.80	37.87	28.23	32.60	39.97	33.35	32.70
NMF-LP [47]	31.30	43.93	33.40	30.57	34.87	30.93	31.03	34.33	29.47	32.23	43.93	33.21	31.77
ZAC [48]	20.13	20.33	20.20	20.27	20.40	20.23	20.30	20.33	20.43	20.20	20.43	20.28	20.29
DEC [24]	31.17	43.97	29.97	30.60	34.87	28.50	33.40	20.07	29.87	31.97	43.97	31.44	30.89
<i>k</i> -meansNet	33.00	45.00	35.53	31.27	35.33	31.80	36.43	40.63	29.53	33.77	45.00	35.23	34.55

TABLE 3
Clustering **Accuracy** (%) on the last 10 supersets of the **CIFAR100** data set.

Methods	s11	s12	s13	s14	s5	s16	s17	s18	s19	s20	max	mean	median
<i>k</i> -means	39.53	28.37	25.23	26.87	24.10	31.83	27.50	32.83	31.00	39.80	39.80	30.71	29.69
FCM [44]	41.80	29.33	23.77	26.77	23.30	29.40	27.43	23.27	25.70	32.97	41.80	28.37	27.10
SC [7]	40.77	31.80	24.83	26.33	23.97	31.03	30.57	30.97	28.50	39.30	40.77	30.81	30.77
LRR [11]	21.87	21.67	21.97	21.67	20.37	21.27	21.77	22.00	21.20	21.47	22.00	21.53	21.67
LSR1 [13]	21.80	21.93	21.57	21.30	22.10	22.27	22.00	21.70	21.60	21.90	22.27	21.82	21.85
LSR2 [13]	26.43	22.13	20.30	24.10	22.00	21.97	21.47	21.07	21.17	24.60	26.43	22.52	21.99
SLRR [27]	22.63	22.50	22.03	22.90	22.27	21.57	21.47	22.77	23.30	22.37	23.30	22.38	22.44
LSC-R [46]	41.53	30.87	24.47	26.43	23.70	20.97	29.10	31.97	28.63	32.93	41.53	29.06	28.87
LSC-K [46]	43.90	30.67	24.67	26.57	24.10	29.10	30.77	30.37	29.57	38.60	43.90	30.83	29.97
NMF-LP [47]	42.00	30.27	25.00	25.33	22.83	30.33	29.13	32.13	29.13	40.97	42.00	30.71	29.70
ZAC [48]	20.20	20.23	20.30	20.27	20.23	20.30	20.30	20.27	20.23	20.23	20.30	20.26	20.25
DEC	21.80	20.17	25.03	26.90	23.80	31.83	27.07	28.57	30.63	41.17	41.17	27.70	26.99
<i>k</i> -meansNet	44.20	32.23	25.87	27.50	24.80	33.60	31.33	34.10	30.00	43.17	44.20	32.68	31.78

In the following section, we will show that *k*-meansNet will further improve the state of the art if other feature extractors such as CNN are used.

Like CIFAR-10, the CIFAR100 dataset also includes 60,000 images. The difference between them is that CIFAR100 includes 100 subjects which could be further grouped into 20 superclasses each of which consists of 3000 samples. Noted that, CIFAR10 and CIFAR100 are more challenging than the mnist dataset, which are less investigated in prior clustering works.

Tables 2–3 show the clustering result of our method on 20 subsets of CIFAR100. Again, the proposed *k*-meansNet

shows promising results on the data sets, which is 1.88% and 1.85% at least higher than the other methods in terms of mean Accuracy on the first and last 10 subsets. Comparing with the recently proposed DEC, our method earns a performance gain of 3.79% and 4.98% on the first and last 10 subsets, respectively. Moreover, *k*-meansNet remarkably outperforms *k*-means and FCM by a considerable margin in mean Accuracy. More specifically, the gains over *k*-means are 2.05% and 1.87%, and that over FCM are 6.07% and 4.31%.

4.3 Influence of Parameters

In this section, we investigate the influence of the parameter α on the mnist data set. In experiment, we increase the value of α from 10^{-5} to 0.5 as shown in Fig. 3. From the result, one could find that the proposed k -meansNet achieves stable clustering result in general. The Accuracy, NMI, and ARI usually change around 85%, 77%, and 75%.

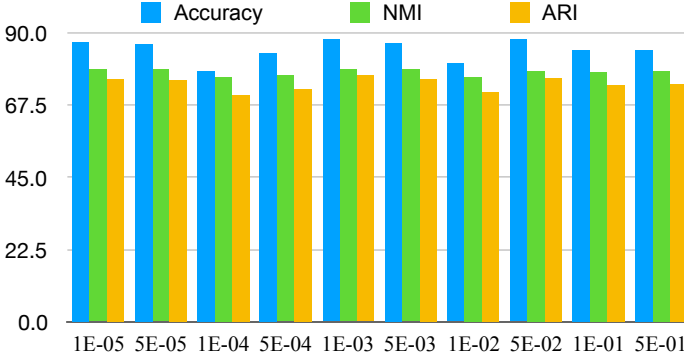


Fig. 3. Influence of the parameter α .

4.4 Influence of Initializations, Features, and Optimizers

As discussed in Introduction, the center-based clustering method is sensitive to the initial clustering centers. In this section, we examine the influence of three different initialization methods, namely, k -means++, k -means, and random method. Besides the performance with fully connected auto-encoder as aforementioned, we also investigate the performance of our method by collaborating with a convolutional auto-encoder. More specifically, the used convolutional encoder is a six-layer network which is with conv(64,5)-pool(2)-conv(32,5)-pool(2)-FCL(1024)-FCL(10), where “conv(64,5)” denotes a convolutional layer with the filter size of 64 and the kernel size of 5, “pool(5)” denotes max-pooling operation with the kernel size of 2, and “FCL(1024)” is a fully connected layer with 1024 neurons. The decoder is symmetric to the encoder. Similar to fully connected auto-encoder, *ReLU* is used as the activation function for all layers except the last one of encoder and decoder which adopts the *sigmoid* function. The experiments are conducted on mnist and k -means is used as the baseline. Furthermore, α of k -meansNet is fixed to 10^{-2} for the convolutional case and 10^{-3} for fully connected case.

From Table 4, we have following observations. First, the proposed k -meansNet is robust to the choice of initialization method. In the case of FCN, it almost keeps unchanged. For CNN, the difference between the maximal and minimal Accuracy is about 2%, and this gaps in NMI and ARI are 1.7% and 2.98%. Second, our method benefits much more from CNN than k -means. For example, our method improves the Accuracy by 3.46% versus 1.66% given by k -means.

Besides the above investigation on different initializations and features, we also consider the role of the used optimization approaches. In our experiments, we carry out experiments on the mnist dataset with the aforementioned CNN network and employ four popular SGD variants,

namely, adadelta [49], adagrad [52], adam [53], and RM-Sprop [54], to train k -meansNet. In the evaluation, we adopt the default setting for these optimizers and experimentally set α to 10^{-2} for adadelta and adam, and to 10^{-3} for adagrad and RMSprop. For a more comprehensive study, we further adopt four metrics for evaluating the clustering quality, *i.e.*, adjusted mutual index (AMI), Homogeneity, Completeness, and v _measure. Noticed that, Accuracy, AMI, ARI, and AMI are external metrics which are computed based on the ground-truth, whereas Homogeneity, Completeness, and v _measure are internal metrics which measure the compactness/scatterness of within-/between-clusters. From TABLE 5, it is easy to observe that AdaDelta and Adam achieve the best performance in terms the used metrics, and Adagrad performs the worst. Such a result is consistent with the experimental results of prior works.

4.5 Convergence Analysis in Experiments

In Section 3.2, we have theoretically shown that our method will sufficiently approximate to the global optimum under some mild conditions. In this Section, we conduct experiments on the mnist dataset to verify our theoretical result. In Fig. 4, we report the clustering results and the loss value of our method with the fully connected neural network and the convolutional neural network which are presented in Section 4.4. From the result, ones could observe that k -meansNet achieves convergence after ~ 1700 epochs in terms of Accuracy, NMI, ARI, and the loss value. Considering the difference in k -meansNet with FCN and with CNN, the former gives slightly changed results after 1650 epochs, whereas the latter keeps stability after 1550. For example, the Accuracy of k -meansNet with FCN ranges from 84.37% to 88.09% after 1650 epochs, and the range of k -meansNet with CNN is [91.04%, 93.96%] after 1550 epochs.

5 CONCLUSION

In this paper, we proposed a novel neural network which is derived from the vanilla k -means clustering algorithm from the standpoint of differentiable programming. Besides proposing a neural network based clustering method, we contribute to differentiable programming in following two aspects. On the one hand, existing works in differentiable programming employ neural networks as an alternative optimization method, whereas we use neural networks to directly describe physical models. On the other hand, the pioneer works in differentiable programming obtained a recurrent neural network, whereas our obtain a feedforward neural network.

ACKNOWLEDGMENT

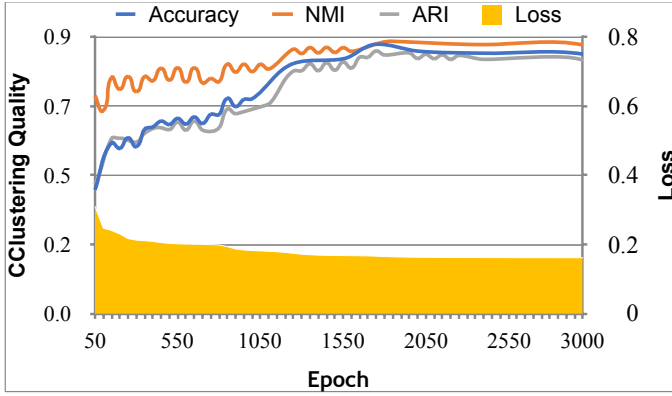
The authors would like to thank the Associate Editor and anonymous reviewers for their future valuable comments and constructive suggestions, and also thank Huan Li and Prof. Zhouchen Lin to provide helps and insights in theoretical analysis, especially the analysis on decoupling on \mathbf{W} and \mathbf{b} .

TABLE 4
Influence of different initialization methods and different features on the **mnist** data set.

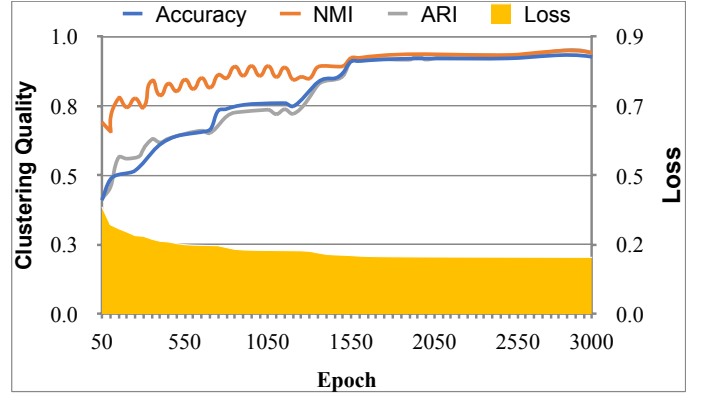
Methods	Initializations	Raw Data			FCN			CNN		
		Accuracy	NMI	ARI	Accuracy	NMI	ARI	Accuracy	NMI	ARI
<i>k</i> -means	random	54.23%	48.49%	36.50%	77.31%	76.71%	69.48%	78.98%	77.45%	72.16%
	<i>k</i> -means++	53.24%	49.98%	36.52%	78.32%	77.75%	70.53%	79.98%	79.46%	73.16%
<i>k</i> -meansNet	random	57.31%	51.14%	38.89%	87.72%	78.26%	75.91%	93.20%	85.51%	85.66%
	<i>k</i> -means++	57.55%	50.31%	38.90%	87.76%	78.70%	76.21%	91.26%	83.81%	82.68%
	<i>k</i> -means	58.08%	51.21%	39.66%	87.56%	78.70%	76.06%	92.42%	84.70%	84.27%

TABLE 5
Influence of different optimizers on the **mnist** dataset.

Optimizers	Accuracy	NMI	ARI	AMI	Homogeneity	Completeness	v_measure
AdaDelta	93.11%	85.52%	85.54%	85.47%	85.48%	85.55%	85.52%
Adagrad	61.09%	71.55%	56.11%	65.03%	65.04%	78.71%	71.22%
Adam	92.13%	84.23%	83.72%	84.18%	84.18%	84.27%	84.23%
RMSprop	80.08%	79.69%	73.38%	79.03%	79.04%	80.35%	79.69%



(a) *k*-meansNet with FCN.



(b) *k*-meansNet with CNN.

Fig. 4. Performance v.s. Training Epoch on the mnist dataset. The left and right y-axis denote the clustering result and the loss, respectively.

REFERENCES

- [1] A. K. Jain, M. N. Murty, and P. J. Flynn, "Data clustering: A review," *ACM Comput. Surv.*, vol. 31, no. 3, pp. 264–323, Sep. 1999. **1**
- [2] R. Vidal, "Subspace clustering," *IEEE Signal Proc. Mag.*, vol. 28, no. 2, pp. 52–68, 2011. **1**
- [3] J. P. Costeira and T. Kanade, "A multibody factorization method for independently moving objects," *Int. J. Comput. Vis.*, vol. 29, no. 3, pp. 159–179, 1998. **1**
- [4] R. Vidal, Y. Ma, and S. Sastry, "Generalized principal component analysis (GPCA)," *IEEE Trans. Pattern Anal. Mach. Intell.*, vol. 27, no. 12, pp. 1945–1959, 2005. **1**
- [5] P. S. Bradley and O. L. Mangasarian, "k-plane clustering," *J. Global Optim.*, vol. 16, no. 1, pp. 23–32, 2000. **1**
- [6] S. Rao, R. Tron, R. Vidal, and Y. Ma, "Motion segmentation via robust subspace separation in the presence of outlying, incomplete, or corrupted trajectories," in *Proc. of 21th IEEE Conf. Comput. Vis. and Pattern Recognit.*, Anchorage, AL, Jun. 2008, pp. 1–8. **1**
- [7] A. Y. Ng, M. I. Jordan, and Y. Weiss, "On spectral clustering: Analysis and an algorithm," in *Proc. of 14th Adv. in Neural Inf. Process. Syst.*, Vancouver, Canada, Dec. 2001, pp. 849–856. **1, 5, 6**
- [8] J. B. Shi and J. Malik, "Normalized cuts and image segmentation," *IEEE Trans. Pattern Anal. Mach. Intell.*, vol. 22, no. 8, pp. 888–905, 2000. **1**
- [9] E. Elhamifar and R. Vidal, "Sparse subspace clustering: Algorithm, theory, and applications," *IEEE Trans. Pattern Anal. Mach. Intell.*, vol. 35, no. 11, pp. 2765–2781, 2013. **1, 2**
- [10] Y. Yang, J. Feng, N. Jojic, J. Yang, and T. S. Huang, "Subspace learning by l0-induced sparsity," *International Journal of Computer Vision*, Jul 2018. [Online]. Available: <https://doi.org/10.1007/s11263-018-1092-4> **1, 2**
- [11] G. Liu, Z. Lin, S. Yan, J. Sun, Y. Yu, and Y. Ma, "Robust recovery of subspace structures by low-rank representation," *IEEE Trans. Pattern Anal. Mach. Intell.*, vol. 35, no. 1, pp. 171–184, 2013. **1, 2, 5, 6**
- [12] P. Favaro, R. Vidal, and A. Ravichandran, "A closed form solution to robust subspace estimation and clustering," in *Proc. of 24th IEEE Conf. Comput. Vis. and Pattern Recognit.*, Colorado Springs, CO, Jun. 2011, pp. 1801–1807. **1, 2**
- [13] C. Lu, H. Min, Z. Zhao, L. Zhu, D. Huang, and S. Yan, "Robust and efficient subspace segmentation via least squares regression," in *Proc. of 12th Eur. Conf. Comput. Vis.*, Florence, Italy, Oct. 2012, pp. 347–360. **1, 2, 5, 6**
- [14] C. You, C. G. Li, D. P. Robinson, and R. Vidal, "Oracle based active set algorithm for scalable elastic net subspace clustering," in *Proc. of 29th IEEE Conf. Comput. Vis. and Pattern Recognit.*, Las Vegas, NV, Jun. 2016, pp. 3928–3937. **1, 2**
- [15] V. Patel, H. V. Nguyen, and R. Vidal, "Latent space sparse subspace clustering," in *Proc. of 14th IEEE Conf. Comput. Vis.*, Sydney, VIC, Dec. 2013, pp. 225–232. **1, 2**
- [16] C. Zhang, H. Fu, S. Liu, G. Liu, and X. Cao, "Low-Rank Tensor Constrained Multiview Subspace Clustering," in *Proc. of 21th Int. Conf. Comput. Vis.* Santiago: IEEE, Dec. 2015, pp. 1582–1590. **1, 2**
- [17] Y. Yang, J. Feng, N. Jojic, J. Yang, and T. S. Huang, "L0-sparse subspace clustering," in *Proc. of 14th Euro. Conf. Comput. Vis.*, Amsterdam, Netherlands, Oct. 2016, pp. 731–747. **1**
- [18] D. Park, C. Caramanis, and S. Sanghavi, "Greedy subspace clustering," in *Proceedings of the 27th International Conference on Neural*

Information Processing Systems - Volume 2, ser. NIPS'14, Cambridge, MA, USA, 2014, pp. 2753–2761. **1**

- [19] Y.-X. Wang, H. Xu, and C. Leng, "Provable subspace clustering: When lrr meets ssc," in *Advances in Neural Information Processing Systems*, C. J. C. Burges, L. Bottou, M. Welling, Z. Ghahramani, and K. Q. Weinberger, Eds., 2013, pp. 64–72. **1**
- [20] Q. W. M. Chen and X. Li, "Robust adaptive sparse learning method for graph clustering," in *IEEE International Conference on Image Processing*. **1**
- [21] C. Lu, J. Feng, Z. Lin, T. Mei, and S. Yan, "Subspace clustering by block diagonal representation," *IEEE Transactions on Pattern Analysis and Machine Intelligence*, pp. 1–1, 2018. **1**
- [22] M. Belkin and P. Niyogi, "Laplacian eigenmaps for dimensionality reduction and data representation," *Neural Comput.*, vol. 15, no. 6, pp. 1373–1396, 2003. **1**
- [23] X. Peng, S. Xiao, J. Feng, W. Yau, and Z. Yi, "Deep subspace clustering with sparsity prior," in *Proc. of 25th Int. Joint Conf. Artif. Intell.*, New York, NY, USA, Jul. 2016, pp. 1925–1931. **1, 2**
- [24] J. Xie, R. Girshick, and A. Farhadi, "Unsupervised deep embedding for clustering analysis," in *Proc. of 33th Int. Conf. Mach. Learn.*, New York, Jun. 2016. **1, 5, 6**
- [25] J. Yang, D. Parikh, and D. Batra, "Joint unsupervised learning of deep representations and image clusters," in *Proc. of 29th IEEE Conf. Comput. Vis. and Pattern Recognit.*, 2016. **1**
- [26] P. Ji, T. Zhang, H. Li, M. Salzmann, and I. Reid, "Deep subspace clustering networks," in *Proc. of 29th Adv. in Neural Inf. Process. Syst.*, Montreal, Canada, Dec. 2017. **1, 2**
- [27] X. Peng, H. Tang, L. Zhang, Z. Yi, and S. Xiao, "A unified framework for representation-based subspace clustering of out-of-sample and large-scale data," *IEEE Transactions on Neural Networks and Learning Systems*, vol. PP, no. 99, pp. 1–14, 2015. **1, 5, 6**
- [28] Y. Bengio, A. Courville, and P. Vincent, "Representation learning: A review and new perspectives," *IEEE Trans. Pattern Anal. Mach. Intell.*, vol. 35, no. 8, pp. 1798–1828, Aug. 2013. **2**
- [29] K. Gregor and Y. LeCun, "Learning fast approximations of sparse coding," in *Proc. of 27th Int. Conf. Mach. Learn.*, USA, 2010, pp. 399–406. **2, 3**
- [30] Z. Wang, S. Chang, J. Zhou, M. Wang, and T. S. Huang, "Learning a task-specific deep architecture for clustering," in *Proc. of SIAM Int. Conf. on Data Mining*, Miami, Florida, May 2015, pp. 369–377. **2, 3**
- [31] W. Zuo, D. Ren, D. Zhang, S. Gu, and L. Zhang, "Learning Iteration-wise Generalized Shrinkage-Thresholding Operators for Blind Deconvolution," *IEEE Trans. Image Process.*, vol. 25, no. 4, pp. 1751–1764, 2016. **2, 3**
- [32] P. Sprechmann, A. M. Bronstein, and G. Sapiro, "Learning efficient sparse and low rank models," *IEEE Transactions on Pattern Analysis and Machine Intelligence*, vol. 37, no. 9, pp. 1821–1833, Sep. 2015. **2, 3**
- [33] S. Zheng, S. Jayasumana, B. Romera-Paredes, V. Vineet, Z. Su, D. Du, C. Huang, and P. H. S. Torr, "Conditional random fields as recurrent neural networks," in *Proc. of 21th Int. Conf. Comput. Vis.*, Santiago, Chile, Dec 2015, pp. 1529–1537. **2, 3**
- [34] R. Liu, G. Zhong, J. Cao, Z. Lin, S. Shan, and Z. Luo, "Learning to diffuse: A new perspective to design pdes for visual analysis," *IEEE Trans. Pattern Anal. Mach. Intell.*, vol. 38, no. 12, pp. 2457–2471, Dec 2016. **2, 3**
- [35] F. Wang, X. Wu, G. M. Essertel, J. M. Decker, and T. Rompf, "Demystifying differentiable programming: Shift/reset the penultimate backpropagator," *CoRR*, vol. abs/1803.10228, 2018. [Online]. Available: <http://arxiv.org/abs/1803.10228> **2**
- [36] X. Peng, Z. Yu, Z. Yi, and H. Tang, "Constructing the l2-graph for robust subspace learning and subspace clustering," *IEEE Trans. Cybern.*, vol. 47, no. 4, pp. 1053–1066, Apr. 2017. **2**
- [37] S. Xiao, M. Tan, D. Xu, and Z. Dong, "Robust kernel low-rank representation," *IEEE Trans. Neural. Netw. Learn. Syst.*, vol. PP, no. 99, pp. 1–1, 2015. **2**
- [38] C. G. Li, C. You, and R. Vidal, "Structured sparse subspace clustering: A joint affinity learning and subspace clustering framework," *IEEE Transactions on Image Processing*, vol. 26, no. 6, pp. 2988–3001, Jun. 2017. **2**
- [39] H. Hu, Z. Lin, J. Feng, and J. Zhou, "Smooth representation clustering," in *Proc. of 27th IEEE Conf. Comput. Vis. and Pattern Recognit.*, Columbus, OH, Jun. 2014, pp. 3834–3841. **2**
- [40] T. Blumensath and M. E. Davies, "Iterative thresholding for sparse approximations," *Journal of Fourier Analysis and Applications*, vol. 14, no. 5, pp. 629–654, 2008. **3**
- [41] Y. Chen, W. Yu, and T. Pock, "On learning optimized reaction diffusion processes for effective image restoration," in *Proc. of 28th IEEE Conf. Comput. Vis. and Pattern Recognit.*, Boston, MA, Jun. 2015, pp. 5261–5269. **3**
- [42] D. Arthur and S. Vassilvitskii, "K-means++: The advantages of careful seeding," in *Proc. of 18th Annual ACM-SIAM Symposium on Discrete Algorithms*, Philadelphia, PA, USA, 2007, pp. 1027–1035. **3**
- [43] J. C. Dunn, "A fuzzy relative of the isodata process and its use in detecting compact well-separated clusters," *Journal of Cybernetics*, vol. 3, no. 3, pp. 32–57, 1973. **3**
- [44] J. C. Bezdek, *Pattern Recognition with Fuzzy Objective Function Algorithms*. Norwell, MA, USA: Kluwer Academic Publishers, 1981. **3, 5, 6**
- [45] S. Boyd, L. Xiao, and A. Mutapcic, "Subgradient methods," *lecture notes of EE392o, Stanford University, Autumn Quarter*, vol. 2004, pp. 2004–2005, 2003. **4**
- [46] D. Cai and X. Chen, "Large scale spectral clustering via landmark-based sparse representation," *IEEE Trans. on Cybern.*, vol. 45, no. 8, pp. 1669–1680, Aug 2015. **5, 6**
- [47] D. Cai, X. He, and J. Han, "Locally consistent concept factorization for document clustering," *IEEE Trans. Knowl. Data Eng.*, vol. 23, no. 6, pp. 902–913, Jun. 2011. **5, 6**
- [48] D. Zhao and X. Tang, "Cyclizing clusters via zeta function of a graph," in *Proc. of 21th Adv. in Neural Inf. Process. Syst.*, Vancouver, Canada, Dec. 2009, pp. 1953–1960. **5, 6**
- [49] M. D. Zeiler, "ADADELTA: an adaptive learning rate method," *CoRR*, vol. abs/1212.5701, 2012. [Online]. Available: <http://arxiv.org/abs/1212.5701> **5, 7**
- [50] Y. Lecun, L. Bottou, Y. Bengio, and P. Haffner, "Gradient-based learning applied to document recognition," *Proc. of IEEE*, vol. 86, no. 11, pp. 2278–2324, Nov. 1998. **5**
- [51] A. Krizhevsky and G. Hinton, "Learning multiple layers of features from tiny images," 2009. **5**
- [52] J. Duchi, E. Hazan, and Y. Singer, "Adaptive subgradient methods for online learning and stochastic optimization," *Journal of Machine Learning Research*, vol. 12, no. Jul, pp. 2121–2159, 2011. **7**
- [53] D. Kingma and J. Ba, "Adam: A method for stochastic optimization," in *Proc. of 3th Int. Conf. Learn Rep.*, 2015, pp. 1–15. **7**
- [54] T. Tieleman and G. Hinton, "Lecture 6.5-rmsprop: Divide the gradient by a running average of its recent magnitude," *COURSERA: Neural networks for machine learning*, vol. 4, no. 2, pp. 26–31, 2012. **7**



Xi Peng received the Ph.D. degree in Computer Science from the Sichuan University in 2013. He currently is a research professor with the College of Computer Science, Sichuan University, Chengdu, China. From 2014 to 2017, he was a research scientist at Institute for Infocomm, Research Agency for Science, Technology and Research (A*STAR) Singapore. His current research interests include machine intelligence and has co-authored more than 40 articles in these areas.

Dr. Peng has served as an Associate/Guest Editor for *IEEE Access*, *IEEE Trans. on Neural Network and Learning Systems*, *Image and Vision Computing* and *IET Image Processing*; a Session Chair for AAAI'17 and IJCAI'18; a Senior Program Committee Member for IJCAI'17; a Program Committee Member and a reviewer for over 50 international conferences and international journals. He has been a chair to organize a tutorial at ECCV'16 and a special session at VCIP'17.



Joey Tianyi Zhou is a scientist with Institute of High Performance Computing (IHPC), Research Agency for Science, Technology and Research (A*STAR) Singapore. He was a senior research engineer with SONY US Research Center, USA. He received his Ph.D. degree in computer science from Nanyang Technological University (NTU), Singapore, in 2015. He was awarded the NIPS 2017 Best Reviewer Award, Best Paper Award at the BeyondLabeler workshop on IJCAI 2016, Best Paper Nomination at ECCV 2016 and

Best Poster Honorable Mention at ACML 2012. His research interests include transfer learning and sparse coding.



Hongyuan Zhu (S'13–M'14) received the B.S. degree in software engineering from the University of Macau, Macau, China, in 2010, and the Ph.D. degree in computer engineering from Nanyang Technological University, Singapore, in 2014. He is currently a Research Scientist with the Institute for Infocomm Research, A*STAR, Singapore. His research interests include multimedia content analysis and segmentation, specially image segmentation/cosegmentation, object detection, scene recognition, and saliency

detection.